Sørensen, M., Stromeyer, D., Grünthal, G. (2010): A macroseismic intensity prediction equation for intermediate depth earthquakes in the Vrancea region, Romania. - Soil Dynamics and Earthquake Engineering, 30, 11, 1268-1278

DOI: 10.1016/j.soildyn.2010.05.009

Soil Dynamics and Earthquake Engineering 30 (2010) 1268-1278

A macroseismic intensity prediction equation for intermediate depth earthquakes in the Vrancea region, Romania

Mathilde B. Sørensen*, Dietrich Stromeyer, Gottfried Grünthal

GFZ German Research Centre for Geosciences, Section 2.6 Seismic Hazard and Stress Field, Telegrafenberg, 14473 Potsdam

ARTICLE INFO

Article history:
Received 18 November 2009
Received in revised form 20 May 2010
Accepted 24 May 2010

ABSTRACT

The use of shake maps in terms of macroseismic intensity in earthquake early warning systems as well as intensity based seismic hazard assessments provides a valuable supplement to typical studies based on recorded ground motion parameters. A requirement for such applications is ground motion prediction equations (GMPE) in terms of macroseismic intensity, which have the advantages of good data availability and the direct relation of intensity to earthquake damage. In the current study, we derive intensity prediction equations for the Vrancea region in Romania, which is characterized by the frequent occurrence of large intermediate depth earthquakes giving rise to a peculiar anisotropic ground shaking distribution. The GMPE have a physical basis and take the anisotropic intensity distribution into account through an empirical regional correction function. Furthermore, the relations are easy to implement for the user. Relations are derived in terms of epicentral, rupture and Joyner-Boore distance and the obtained relations all provide a new intensity estimate with an uncertainty of ca. 0.6 intensity units.

1. Introduction

The seismic hazard in Romania is dominated by the repeated occurrence of intermediate depth earthquakes in the Vrancea region. These earthquakes are geographically confined to a very limited volume in the depth interval 60-200 km with moment magnitudes reaching 7.9 [1] and are expected to be associated with a partly detached slab under the Carpathian mountain belt. During the last century, four major earthquakes have affected the region (1940: $M_w = 7.7$, 1977: $M_w = 7.4$, 1986: $M_w = 7.1$ and 1990: $M_w = 6.9$ [2]), the 1977 event causing severe damage mainly in Bucharest and killing ca. 1500 people [3].

In such regions of high seismic hazard, an essential parameter is the attenuation of seismic waves which must be known for seismic hazard assessment and when generating shake maps with the purpose of earthquake early warning or rapid earthquake response. Ground motion prediction equations (GMPE), also often referred to as attenuation relations, are traditionally given in terms of recorded ground motion parameters, for example peak ground acceleration (PGA) based on strong motion data. When studying the damage potential of large earthquakes, such PGAbased relations have two drawbacks. First, the availability of recordings is limited and therefore one is often forced to apply GMPE based on recordings from different areas with similar tectonics. Second, there is no straightforward way to associate the recorded ground motions with damage which is a complex function of ground motion level, duration, local site conditions and building vulnerability.

As an alternative, to overcome these problems, ground motion attenuation can be expressed in terms of macroseismic intensity. Intensities have the major advantage of much better availability, as data are dependent on the availability of people and a built environment rather than instrumentation, and therefore can be sampled closer and as far back in time as historical records allow. Furthermore, the macroseismic intensity is assigned based on the observed ground shaking and damage, and thereby it can be directly related to the damage potential of future earthquakes. Another advantage is that intensity data are easy understandable by non-seismologists and easy convertible by risk management teams.

In the present study we derive new GMPE for macroseismic intensity valid for the intermediate depth earthquakes in the Vrancea region, Romania. A peculiar characteristic of the Vrancea earthquakes is the distribution of ground shaking due to the events, which is not symmetric around the rupturing fault plane. There is a systematic shift of the maximum intensities relative to the epicenter and the isoseismal lines are extended further in the NE–SW directions than in the NW–SE directions, indicating stronger attenuation perpendicular to the Carpathian bend than in the parallel direction. This effect has important implications for the seismic hazard related to the Vrancea earthquakes, especially for the city of Bucharest which is in the direction of low attenuation. The distribution can be due to effects of either the earthquake source, the propagation path or the local site conditions. 3D numerical modeling has shown that a combination of basin effects and the radiation pattern caused by the reverse mechanisms of the Vrancea earthquakes can to some extent explain this ground shaking distribution [4]. However, several studies show that regional, frequency dependent differences in attenuation is the most likely cause [5, 6, 7].

Several previous studies have focused on deriving GMPE for macroseismic intensity for the Vrancea

* Corresponding author. Tel.: +49 331 288 1585; fax +49 331 288 1127.
E-mail addresses: sorensen@gfz-potsdam.de (M. B. Sørensen), stro@gfz-potsdam.de (D. Stromeyer), ggrue@gfz-potsdam.de (G. Grünthal)

doi: 10.1016/j.soildyn.2010.05.009

earthquakes, following different approaches to include the anisotropy of attenuation. Most studies have derived several relations valid for different azimuths [8, 9, 10], in some cases including an average relation valid for all azimuths. Alternatively, GMPE have been determined for various characteristic regions by *Sokolov et al.* [11]. *Pantea* [12] follows a combined approach and derives direction dependent GMPE within 8 different zones for shallow Romanian earthquakes. *Ardeleanu et al.* [13, 14], on the other hand, derive a relation which is a simple function of distance, event depth and a correction factor which is determined for a 2D grid covering the studied area. A study of *Zsíros* [15] does not account for the anisotropy of intensity attenuation but presents isotropic relations for fixed epicentral intensities of 7 and 8. Many of the intensity prediction equations available in the literature are highly complex relations for which the physical background in some cases is difficult to justify and which furthermore are complicated to implement for the user. Most relations are based on isoseismal maps and use a point source approximation, not accounting for the extended fault plane due to the Vrancea earthquakes.

The intensity prediction equations presented here are derived following the scheme of *Sørensen et al.* [16], which has been modified to account for the anisotropic intensity distribution characteristic for the Vrancea region. The relations are based on original intensity data points (IDP) from five large Vrancea earthquakes. The obtained GMPE have a physical basis and include anisotropy through a simple two-step relation which is easy to implement for the user.

2. The original attenuation model

We derive GMPE for intermediate depth Vrancea earthquakes based on the model of *Sørensen et al.* [16], which builds on the results of *Stromeyer and Grünthal* [17]. This attenuation model leads to intensity prediction equations that are symmetrical around the rupturing fault plane. In order to account for the anisotropic ground shaking distribution due to the Vrancea earthquakes, a regional correction term is added. In the following, a brief outline is given of the attenuation model as presented by *Sørensen et al.* [16]. The modification of the methodology is described in Section 4.

The attenuation model of *Sørensen et al.* [16] is a physically based relation with the following form:

$$I = cM_w + d\log(h) + e - a\log\sqrt{\frac{R^2+h^2}{h^2}} - b\left(\sqrt{R^2+h^2} - h\right) \quad (1)$$

The first three terms represent the epicentral intensity as a function of moment magnitude (M_w) and depth (h), the fourth and fifth terms represent geometrical spreading (having its main effect at short distances) and energy absorption (most significant at larger distances), respectively. In order to account for the finite dimensions of the fault, R was defined as the Joyner–Boore distance, i.e. the shortest distance to the surface projection of the fault plane, and h as the depth to the center of the fault plane. In the current study, where the considered earthquakes are relatively deep, relations have been derived for Joyner–Boore distance, epicentral distance (assuming a point source with hypocentral depth h) and rupture distance (the shortest distance to the rupturing fault plane), and the results are compared.

Input data for the regression is a collection of intensity data points (IDP) describing the intensity at a given location. To avoid bias due to variation in the number of observations for different intensity classes, a weighting scheme has been applied where each intensity class (integer intensity level) has been assigned the same weight in the regression, regardless of the number of observations within the class. Therefore, the determination of the regression parameters $a, b, \ldots e$ leads to the weighted least squares problem

$$\min_x \|W^{-1}(I - Ax)\|, \quad (2)$$

where $I = (I_i)$, $i = 1, \ldots, n$ is a vector of n IDP, A is an $(n \times 5)$ design matrix, W is an $(n \times n)$ weighting matrix with only diagonal entries and $x = (c, d, e, -a, -b)$ is the parameter vector to be estimated. The values of the diagonal elements of W are chosen in such a way that (1) they are equal for all data in one intensity class and (2) the sum of squared inverse weights is equal for all intensity classes (classes are identically weighted).

3. Data

Regressions have been performed on a dataset covering the latest five large earthquakes with macroseismic intensity data available in the region. These events are listed in Table 1. Maps of macroseismic intensity data points (MSK intensity) have been compiled and digitized by Bonjer in cooperation with Romanian and German scientists. The resulting maps were made available to us as picture files (Bonjer, pers. comm., 2007; Fig. 1). We digitized these maps and obtained a total of 4058 intensity data points for the five earthquakes. The sources have been defined as dipping rectangular faults with location, strike and dip taken from the literature. This information is summarized in Table 2 and the details are described in the following. Isoseismal maps exist for other Vrancea events than the here included, e.g. from *Mândrescu et al.* [18], but have not been used in this study. This has been decided, as the macroseismic intensity data from the older events are associated with large uncertainties, as are the source characteristics of the associated earthquakes. In our opinion, the use of a smaller, but consistent and better constrained dataset will lead to more reliable GMPE.

Table 1
Earthquakes used for deriving GMPE for macroseismic intensity in the Vrancea region. Depth: depth to the upper and the lower edges of the fault plane, M_w: moment magnitude, I_{min}: minimum intensity in dataset, I_{max}: maximum observed intensity.

Event ID	Date	Time	Depth (km)	M_w	I_{min}	I_{max}
1940	10 Nov. 1940	01:39	150–181	7.7	3	9
1977	4 Mar. 1977	19:21	93–131	7.4	4	8
1986	30 Aug. 1986	21:28	125–148	7.1	2	8
1990a	30 May 1990	10:40	73–90	6.9	2	8
1990b	31 May 1990	00:17	84.5–94	6.4	2	7

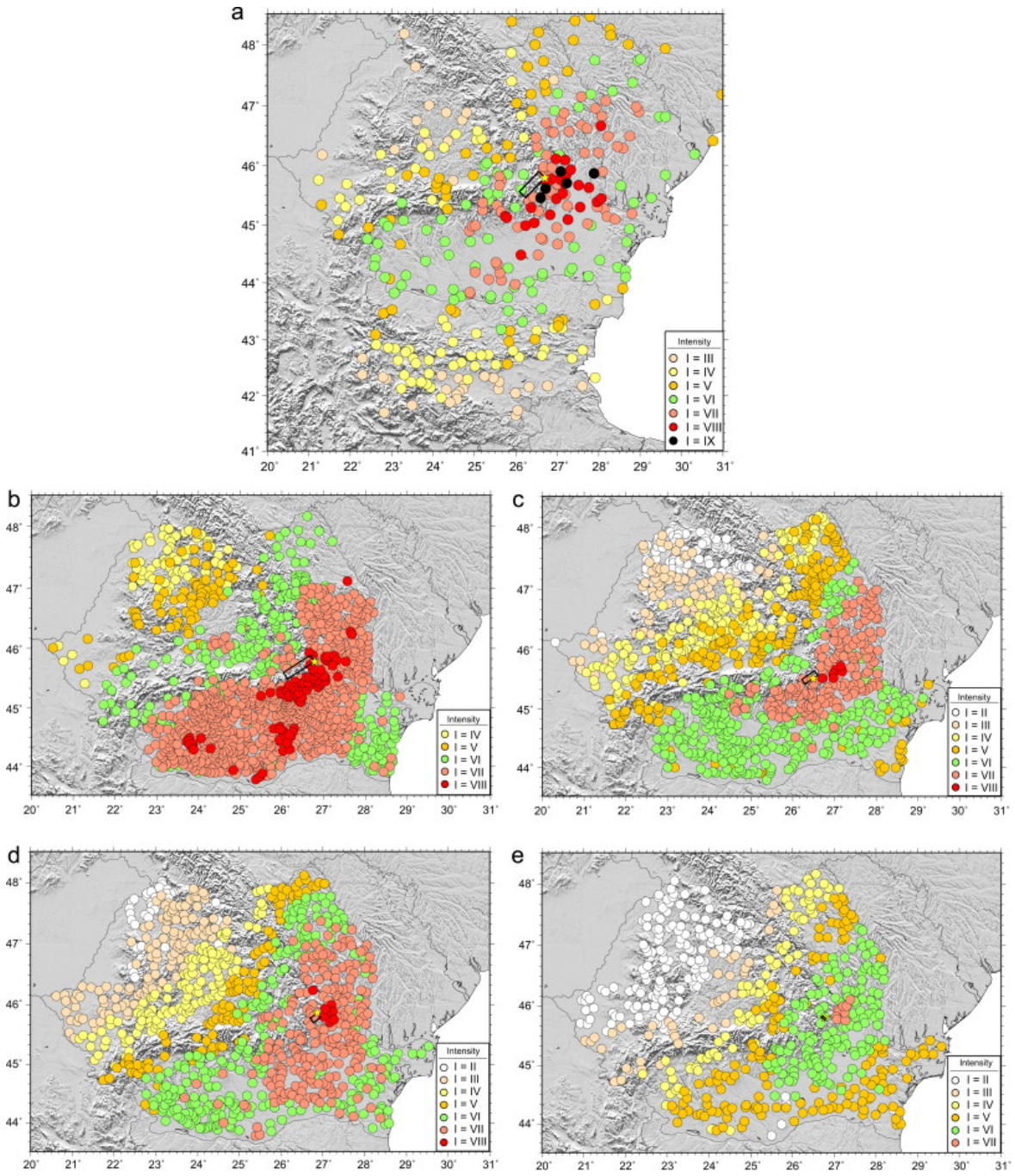

Figure 1. Intensity maps for the five Vrancea earthquakes used in the analysis (data from K.-P. Bonjer, pers. comm. 2007). (a) 1940, (b) 1977, (c) 1986, (d) 1990a and (e) 1990b. Stars indicate epicenters, black boxes outline the surface projections of the fault planes.

For each studied earthquake, the fault plane has been defined based on the location of rupture initiation, strike and dip and the extent of the fault plane as described in the literature. For most events, an estimate of the direction of rupture propagation was also available, making it possible to locate the fault plane relative to the rupture initiation point. The 1940 and 1977 events both ruptured downwards towards SW [19, 20], leading to a location of rupture initiation in the upper northeastern corner of the fault plane. *Trifu and Oncescu* [21] locate the rupture initiation for the 1986 earthquake along the upper edge of the fault plane, 10 km from the north-eastern corner, based on the aftershock distribution. This leads to a bilateral downward rupture propagation. The used location for this event is at some distance from the remaining earthquakes. It is expected that the earthquake was actually located further to the northeast, however we keep the location of *Trifu and Oncescu* [21] for consistency as the shift is in any case at the order of the size of the fault plane and thereby within the expected level of uncertainty in the source location. For the 1990a earthquake, *Oncescu and Bonjer* [19] describe upward propagation of the rupture. We assume the rupture initiation is in the lower northeastern corner of the fault plane. For the 1990b event, we use the source parameters provided by *Perrot et al.* [22] (based on *Tavera* [23]). They describe the rupture to propagate upwards and we assume the rupture to initiate in the centre of the lower edge of the fault plane. The fault dimensions are scaled to half the size of the 1990a event.

The final dataset covers the region between 20.5-30.7°E and 41.7-48.4°N. The studied events have

Table 2
Source parameters of the studied Vrancea earthquakes. Lon: longitude, Lat: latitude, h: hypocenter depth, M_w: moment magnitude, RIP: location of rupture initiation within the fault plane, Length: length of rupturing fault plane along strike, Width: width of rupturing fault plane along dip.

Event ID	Lon	Lat	h	M_w	Strike	Dip	RIP	Length (km)	Width (km)
1940[a]	26.7	45.8	150	7.7	224	62	Upper NE	52	35
1977[b]	26.78	45.78	93	7.4a	237	73	Upper NE	60	40
1986[c]	26.49	45.52	125	7.1a	235	65	Upper, in plane	29	25
1990a[a]	26.87	45.87	90	6.9	232	58	Lower NE	17	20
1990b[d]	26.77	45.81	94	6.4	308	71	Lower centre	9	10

[a] Data from Oncescu and Bonjer [19].
[b] Data from Räkers and Müller [20].
[c] Data from Trifu and Oncescu [21].
[d] Data from Perrot et al. [22] and Tavera [23].

Table 3
Regression parameters for rupture, epicentral and Joyner–Boore distance.

Distance measure	c_1	c_2	c_3	c_4	c_5	c_6
Rupture (Eq. 5)	1.7865	-5.5927	5.9142	-2.2715	-0.0111	0.1408
Epicentral (Eq. 3)	1.9911	-6.6058	6.6081	-3.1223	-0.0085	0.1408
Joyner-Boore (Eq. 3)	1.8872	-6.0793	6.3494	-2.5062	-0.0111	0.1408

Table 4
Regression parameters, p_{ij}, for the regional correction function (4), valid for the rupture distance based relation.

	j=1	j=2	j=3	j=4	j=5
i=1	25.073	23.415	26.135	29.989	27.680
i=2	46.601	44.310	42.955	45.301	46.186
i=3	0.289	0.222	0.233	0.802	0.536
i=4	0.547	1.274	0.731	1.464	0.534
i=5	0.182	0.450	0.078	-0.971	-0.466
i=6	-1.522	1.971	-1.804	1.089	1.073

Table 5
Regression parameters, p_{ij}, for the regional correction function (4), valid for the epicentral distance based relation.

	j=1	j=2	j=3	j=4	j=5
i=1	25.447	23.077	26.279	30.001	27.343
i=2	46.517	44.461	43.107	45.037	45.631
i=3	0.274	0.180	0.279	0.435	0.475
i=4	0.655	1.252	0.691	1.940	0.606
i=5	0.309	0.355	-0.200	-0.892	-0.373
i=6	-1.668	1.833	-1.644	1.277	1.661

Table 6
Regression parameters, p_{ij}, for the regional correction function (4), valid for the Joyner–Boore distance based relation. The spatial distribution of the function is illustrated in Fig. 2.

	j=1	j=2	j=3	j=4	j=5
i=1	25.012	22.899	25.847	29.981	28.202
i=2	46.597	44.514	42.777	45.119	46.301
i=3	0.311	0.262	0.216	0.644	0.342
i=4	0.494	1.355	0.716	1.661	0.862
i=5	0.169	0.484	0.157	-0.869	-0.510
i=6	-1.624	1.863	-1.189	1.077	1.107

magnitudes in the range $M_w = 6.4$–7.7 and ruptured the depth range h = 73-181 km. IDPs are at distances R = 0-520 km from the fault planes. These values set bounds on the validity of the final relations.

4. Modification of the attenuation model

The anisotropic intensity distribution poses challenges in the establishment of a GMPE for the Vrancea region. Several approaches were tested for establishing a relation which fits the intensity distribution, including regression for an elliptically shaped attenuation law with the center shifted relative to the earthquake epicenter. This approach, however, lead to an unstable regression and it proved a better solution to include a regional correction term in the GMPE. Including the correction term, we are searching a relation of the form

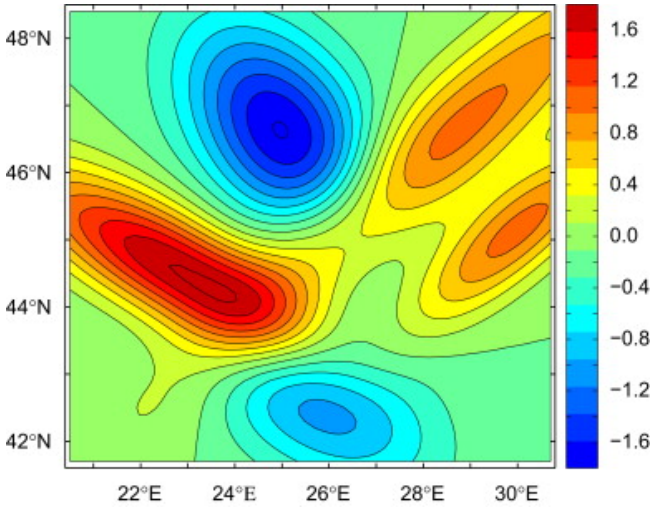

Figure 2. Spatial distribution of the regional correction function (4) for Joyner-Boore distance.

$$I = c_1 M_w + c_2 \log(h) + c_3 + c_4 \log\sqrt{\frac{R^2+h^2}{h^2}} + c_5\left(\sqrt{R^2+h^2}-h\right) + c_6 M_w dl \quad (3)$$

Here, dl is an empirical regional correction function, which is scaled by the earthquake magnitude and a constant c_6, which is chosen so that $c_6 M_{mean} = 1$, where M_{mean} is the average value of magnitude for the included earthquakes (i.e., M_{mean} = 7.1 and c_6 = 0.1408).

Intensity prediction equations are obtained through an iterative procedure in three steps. (1) First, the weighted least-squares regression described in Section 2 is used to derive the isotropic parameters $c_1, \ldots, c_5$ from (3), excluding the dl term. In this way, a relation is obtained which describes the average attenuation, not accounting for anisotropy. (2) The obtained isotropic relation is applied and compared to the observations to derive the residuals for all observations. The residuals are then entered in a nonlinear weighted approximation of dl, using the weights from step (1), to determine the parameters p_{ij} of Eq. (4). (3) The first step is following repeated for the corrected data $I - c_6 M_w dl$ for the final parameters $c_1, \ldots, c_5$. The last step is included to account for the fact that the residuals are only approximated by the regional correction function. By including the last step, all uncertainties are included in the regression for $c_1, \ldots, c_5$.

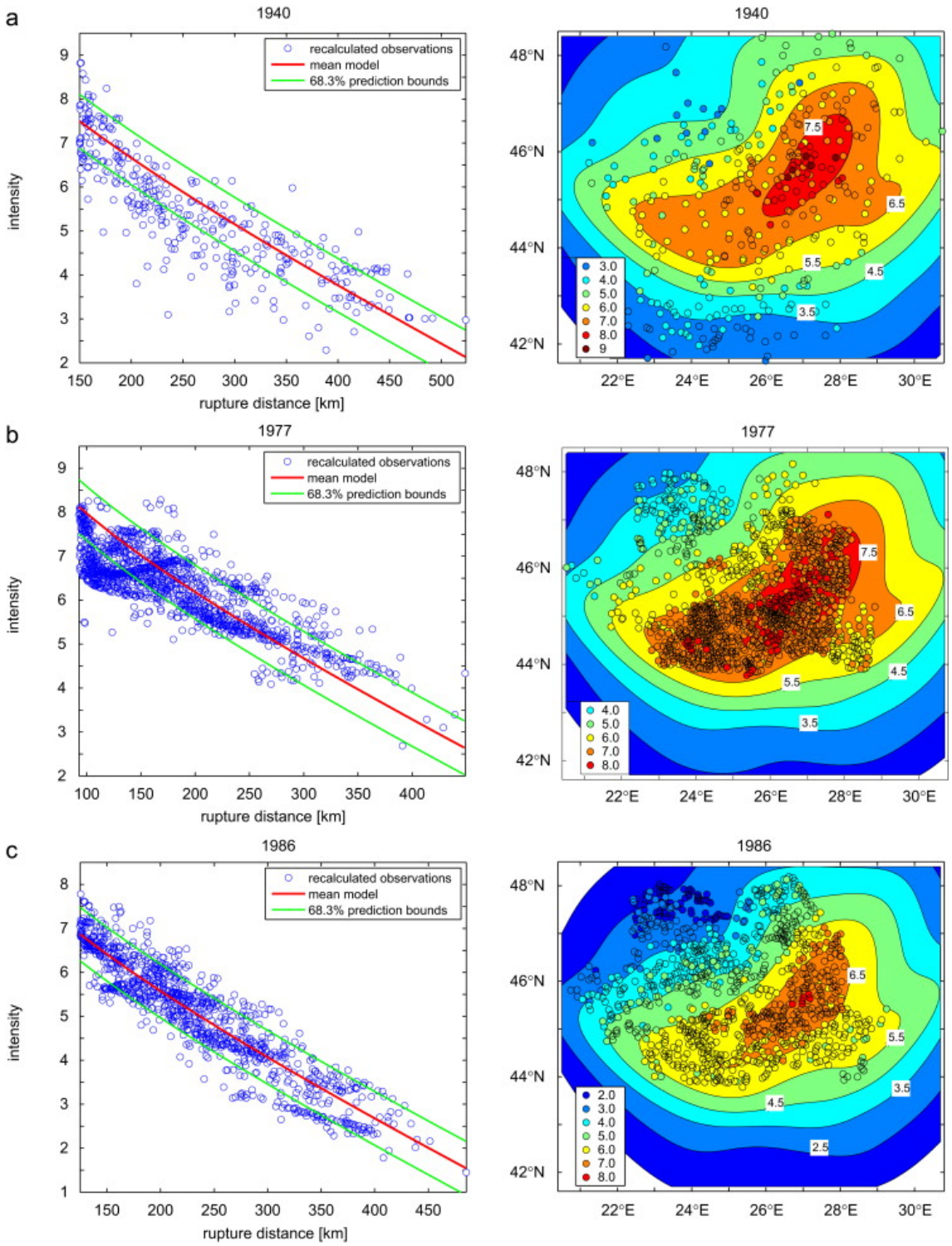

Figure 3. Comparison between observed intensity data (circles) and intensities derived using (5) for rupture distance for the five earthquakes. The left figures show regional corrected intensity vs. distance (see text for details) for the relation (5) (red curve) and the 68.3% prediction bounds (green curves). Regressions are performed for raw data. The right figures show the intensity distribution in a map view. (a) 1940, (b) 1977, (c) 1986, (d) 1990a and (e) 1990b.

Visual inspection of the residuals indicates that there are five regions of extreme values and therefore we choose to define the regional correction function as a spatial function of longitude λ and latitude θ, combining five anisotropic two-dimensional Gaussian-distributed functions:

$$dl(\lambda,\theta) = \sum_{j=1}^{5} p_{6j}\exp\left(-\left[p_{3j}(\lambda - p_{1j})^2 + 2p_{5j}(\lambda - p_{1j})(\theta - p_{2j}) + p_{4j}(\theta - p_{2j})^2\right]\right). \quad (4)$$

In order to test the effect of using different distance measures in the regression for the relatively deep Vrancea earthquakes, we perform three regressions using rupture distance, epicentral distance and Joyner–Boore distance as the distance measure. The epicenter is defined as the surface projection of the rupture initiation point, which is usually the location provided in earthquake catalogs. An important consequence of this definition is that the location of the epicenter with respect to the fault plane varies depending on the

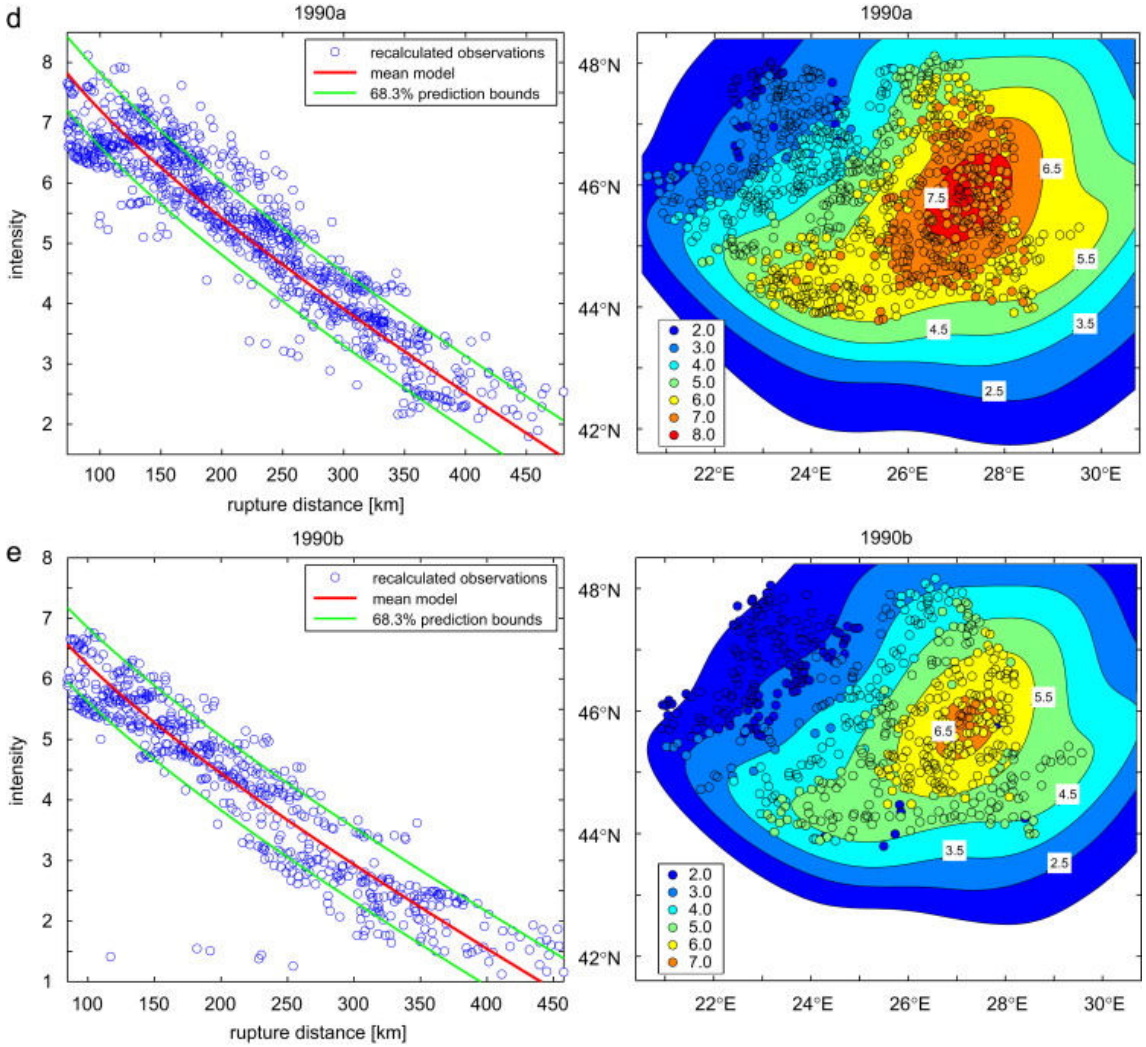

Figure 3. (Continued)

direction of rupture propagation and is therefore different for the considered events. This added variability, however, reflects the common situation when applying the derived relation to an earthquake catalog.

From the initial definition of our GMPE (1), the terms related to $c_1, \ldots, c_2$ represent the epicentral intensity, and consequently the c_4 and c_5 terms should be zero directly above the hypocenter. This requirement is fulfilled when using epicentral distance and Joyner–Boore distance. For rupture distance, on the other hand, the minimum value of R is given by the depth of the upper edge of the fault plane, and these terms will not be zero at the epicenter. To avoid this problem, we modify (3) for the case of rupture distance and use instead

$$I = c_1 M_w + c_2 \log(h) + c_3 + c_4 \log\left(\frac{R}{h}\right) + c_5(R - h) + c_6 M_w dl \quad (5)$$

with $h = \min(R)$.

5. Results

The regression results for $c_1, \ldots, c_6$ are presented in Table 3 for the three distance measures. The parameters for the regional correction function dl are presented in Table 4 for rupture distance, Table 5 for epicentral distance and Table 6 for Joyner–Boore distance. As an example, the spatial distribution of the regional correction function for Joyner–Boore distance is shown in Fig. 2.

Figs. 3-5 show the performances of the relations for the five earthquakes considered in the input data. These figures show a comparison of the IDP to the obtained relations including the 68.3% prediction bounds (corresponding to one standard deviation for normally distributed errors) in a distance vs. intensity plot, as well as a map view comparison of the IDP and contours drawn based on the derived relations. As (3) is not a unique function of distance when including the regional correction term, the distance vs. intensity plots have been created by subtracting the regional correction from the observed data, and comparing these corrected observations to the predictions of (3), excluding the regional correction term. In general, all three relations fit the data well for all earthquakes. This is also clear from Table 7, where the errors in the prediction of a new intensity value (see Sørensen et al. [16] for details) are listed for the three relations for all five earthquakes, as well as the combined error. The combined error is close to 0.6 intensity units for all relations, meaning that

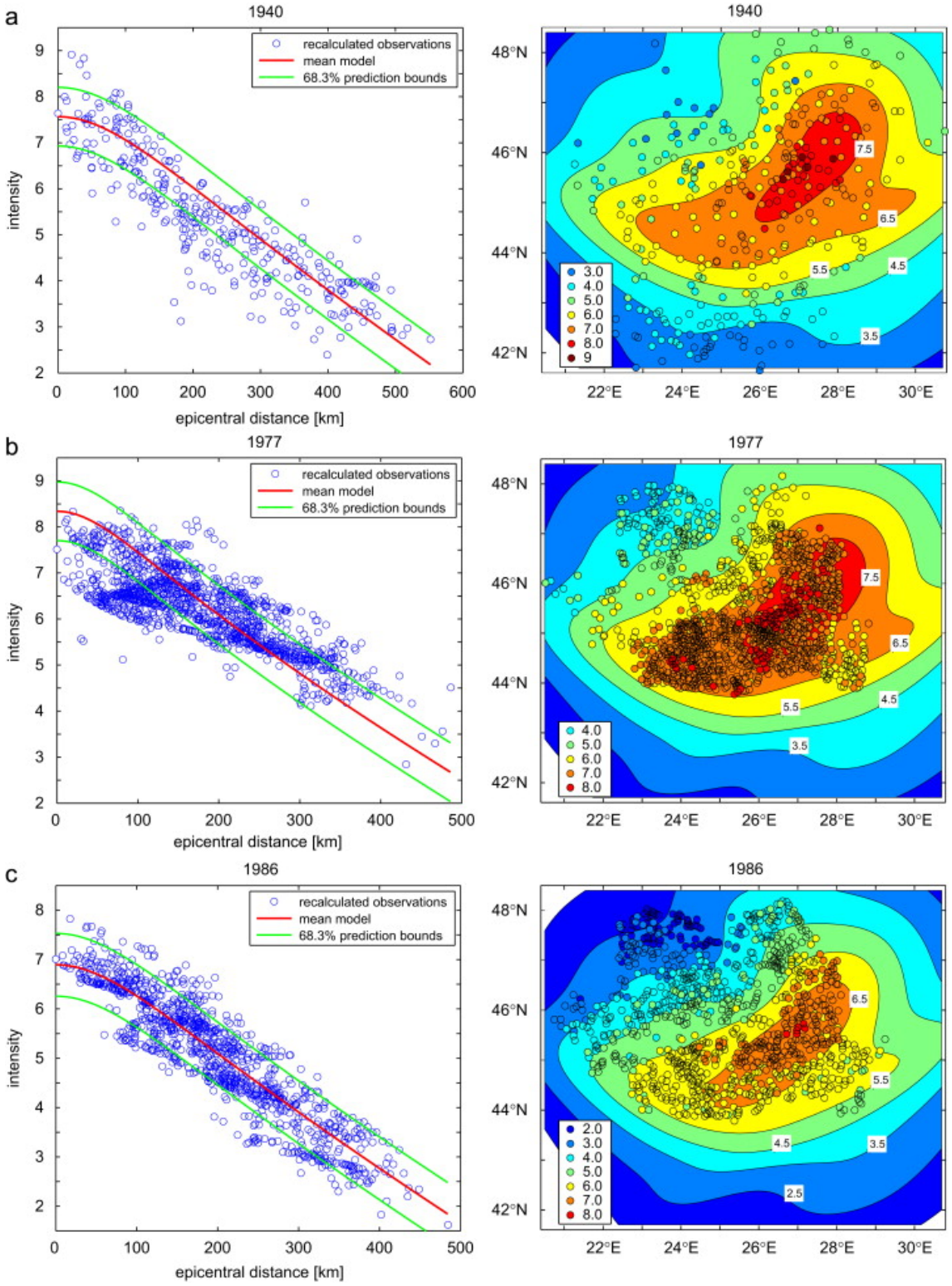

Figure 4. Comparison between observed intensity data (circles) and intensities derived using (3) for epicentral distance for the five earthquakes. The left figures show regional corrected intensity vs. distance (see text for details) for the relation (3) (red curve) and the 68.3% prediction bounds (green curves). Regressions are performed for raw data. The right figures show the intensity distribution in a map view. (a) 1940, (b) 1977, (c) 1986, (d) 1990a and (e) 1990b.

all relations are equally valid and can be applied as most appropriate with the given data at hand.

Maximum and epicentral intensities (which are not necessarily identical due to the regional corrections) of the five input earthquakes have been calculated using the derived GMPE, and are given in Table 8. In general, both epicentral and maximum intensities are well predicted within the uncertainty bounds; however the maximum intensities for the two deeper events (1940 and 1986) are underestimated. It seems that there are effects, not captured in the derived relations, leading to an increased maximum intensity for the deepest Vrancea earthquakes. This could, for example, be due to different rupture propagation on the fault plane or larger stress drop for these events. This theory of differences in the source properties is supported by the

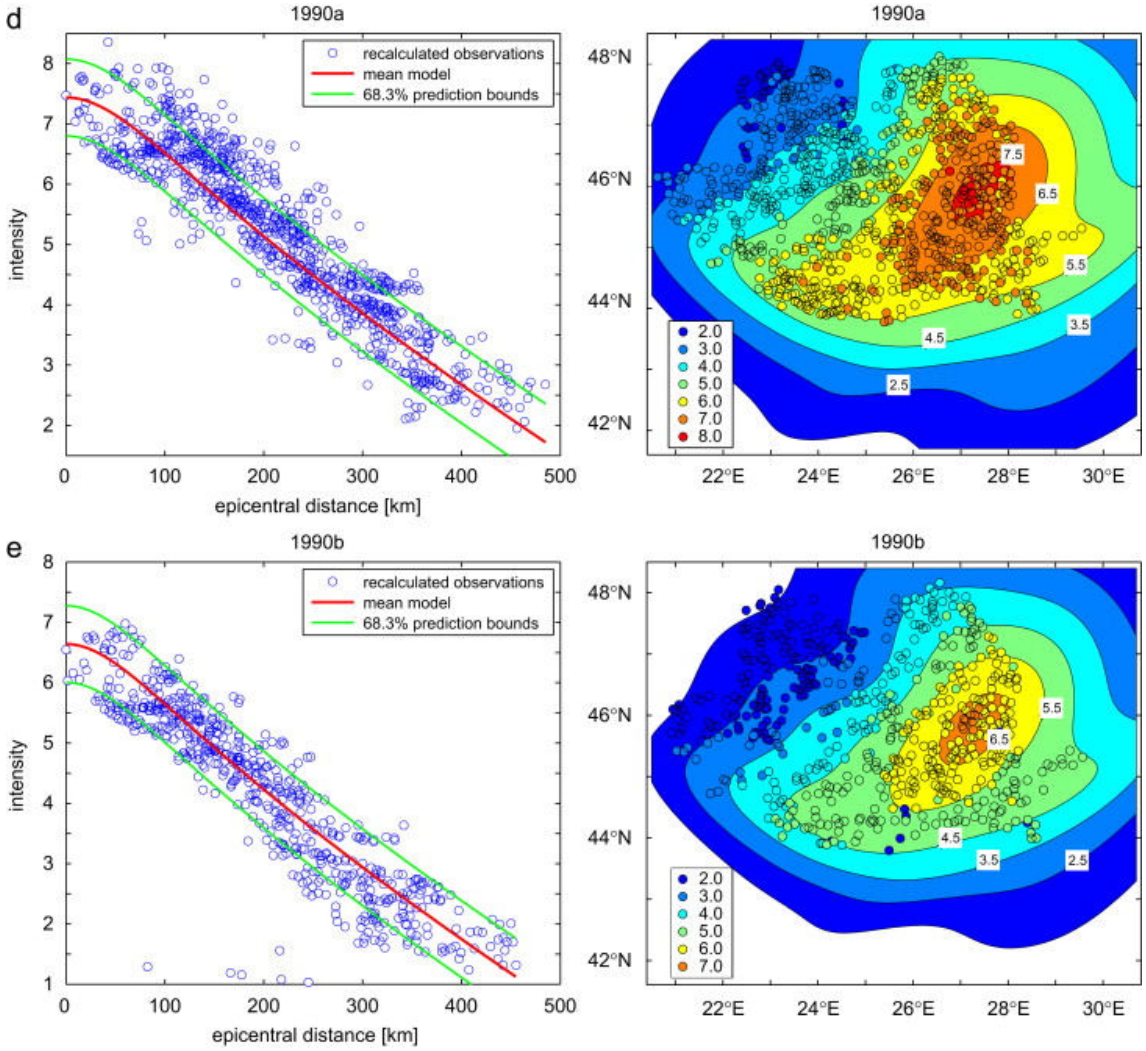

Figure 4. (Continued)

fact that the 1986 earthquake, despite its smaller magnitude and larger depth, gave rise to the same maximum intensity as the 1977 earthquake. Unfortunately, the dataset at hand contains only five earthquakes, and it is not possible to resolve this uncertainty in more detail. Future studies are planned to investigate this phenomenon with the help of synthetic ground motion simulations.

6. Discussion and conclusions

The derived GMPE are based only on the intermediate depth Vrancea earthquakes and are therefore not valid for the shallow, crustal seismicity in Romania. The behavior of the crustal seismicity is expected to be significantly different from that of the intermediate depth events due to the differences in magnitudes and material properties along the wave paths. We would expect a GMPE for the crustal events to be very similar to the one derived for Central Europe by Stromeyer and Grünthal [17]. However, one should keep in mind that whereas the crustal seismicity cannot be neglected in a comprehensive seismic hazard analysis, the Vrancea earthquakes surely represent the greatest seismic hazard for the country.

Based on the definitions of intensity scales it only makes sense to represent intensities as integer values. Our suggestion for dealing with situations where integer values are needed is to apply a simple rounding scheme to the assigned intensities such that e.g. intensities in the interval $4.50 \le I \le 5.49$ are all assigned an intensity value of $I = 5$. This approach has been followed also in Figs. 3–5. Here it is important to keep in mind the difference between calculated and assigned intensities. When assigning intensity values based on macroseismic observations, uncertain observations which can be associated with either of two integer intensity values (e.g. 5 and 6) will usually be assigned the lower intensity value (5) or both values (5–6) [24].

There are several sources of uncertainties associated with the input data used in this analysis. First, the earthquake source parameters, which are taken from the published literature, are in most cases based on limited data, and especially the depths may be debatable. Second, the intensity data are associated with uncertainties related to the subjectivity in intensity assignment and enhanced by the digitization of intensity maps done by the authors. In a recent study [25], we investigated the effect of uncertainties in earthquake source parameters on the regression result when deriving intensity prediction equations. Our results

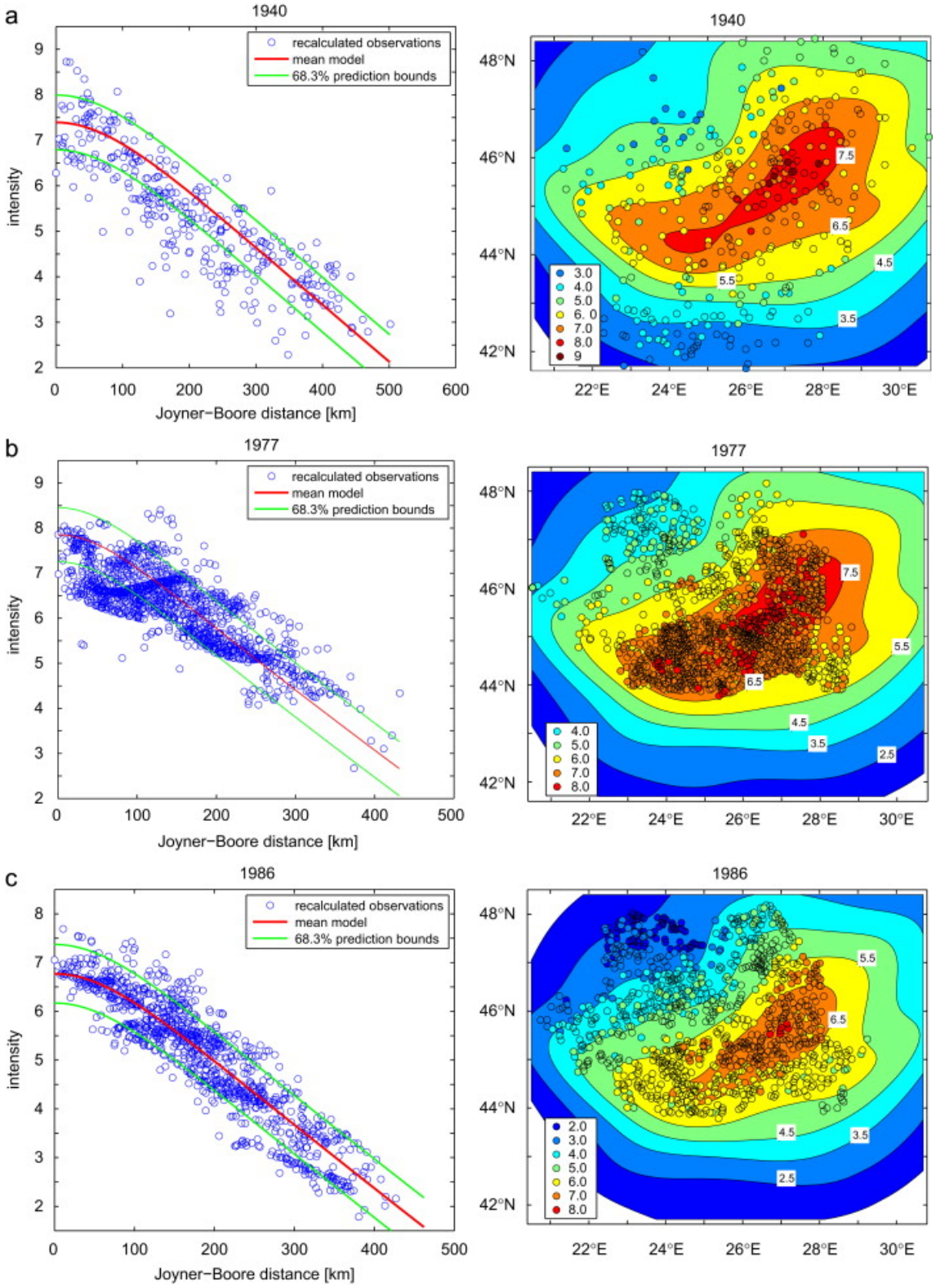

Figure 5. Comparison between observed intensity data (circles) and intensities derived using (3) for Joyner-Boore distance for the five earthquakes. The left figures show regional corrected intensity vs. distance (see text for details) for the relation (3) (red curve) and the 68.3% prediction bounds (green curves). Regressions are performed for raw data. The right figures show the intensity distribution in a map view. (a) 1940, (b) 1977, (c) 1986, (d) 1990a and (e) 1990b.

showed that as long as the intensity data are associated with uncertainties larger than ca. 0.5 intensity units, uncertainties in earthquake source parameters can be neglected. As we expect this to be the case in this study, we have chosen to use fixed values for the earthquake source parameters.

The anisotropic ground shaking distribution due to the Vrancea earthquakes is a peculiarity which is currently not fully understood. There are three main parameters which can cause this pattern: first, the earthquake source and the associated radiation pattern due to reverse faulting on a NW dipping fault plane is consistent with the observed shift of the maximum intensities away from the epicenter. This effect can be

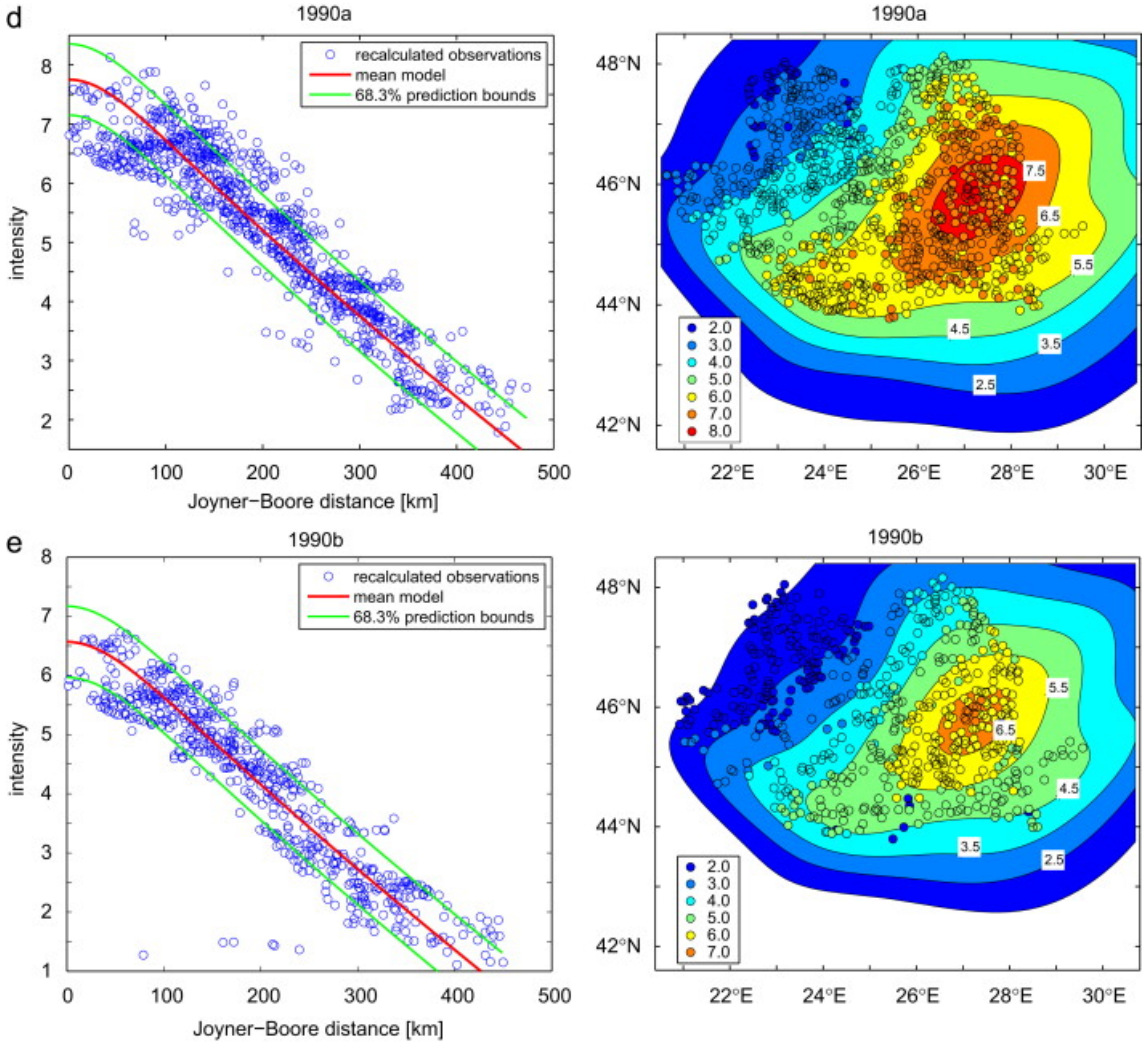

Figure 5. (Continued)

Table 7
Error in a new intensity estimate using relations (3) and (5) for rupture, epicentral and Joyner–Boore distance. Errors for the individual earthquakes as well as an overall error for the combined dataset are given.

Event	Rupture distance	Epicentral distance	Joyner-Boore distance
1940	0.781	0.750	0.797
1977	0.686	0.747	0.644
1986	0.483	0.498	0.495
1990a	0.576	0.583	0.576
1990b	0.581	0.607	0.585
Combined	**0.610**	**0.635**	**0.600**

Table 8
Epicentral and maximum intensities calculated using relations (3) and (5) for rupture, epicentral and Joyner–Boore distance. I_0: epicentral intensity, I_{max}: maximum intensity, RD: rupture distance, ED: epicentral distance, JB: Joyner–Boore distance, Obs: observed.

Event ID	I_0, RD	I_0, ED	I_0, JB	I_0, Obs	I_{max}, RD	I_{max}, ED	I_{max}, JB	I_{max}, Obs
1940	7.50	7.70	7.39	7–8	8.00	8.15	8.01	9
1977	8.13	8.35	7.85	7–8	8.53	8.72	8.38	8
1986	6.87	6.90	6.77	7	7.21	7.22	7.21	8
1990a	7.82	7.41	7.75	7–8	8.24	7.84	8.27	8
1990b	6.57	6.69	6.57	6–7	6.89	6.90	6.97	7

further strengthened by rupture directivity for large earthquakes. Secondly, the tectonic setting and especially the presence of a partly detached slab segment is expected to have significant influence on the wave propagation, leading to large variations in attenuation. Thirdly, local site effects can lead to modifications of ground shaking at a local scale. The relative importance of these factors in the observed ground shaking distribution is under ongoing investigation, but several studies indicate that the variation in attenuation is the most important factor [8, 9, 10]. Whereas this is to be investigated further in the future, we here provide our suggestion for accounting for the anisotropy in intensity prediction equations. The derived relations are applicable for three different distance measures with comparable levels of uncertainty, and are valid in the region 20.5–30.71°E; 41.7–48.4°N, in the magnitude range M_w = 6.4–7.7, in the depth range h = 73–181 km and in the distance range R = 0–520 km.

Acknowledgements

The presented work was carried out as part of the EC funded project SAFER (http://www.saferproject.net). The authors wish to thank K.-P. Bonjer for providing the macroseismic intensity maps used in this study. The thoughtful comments of an anonymous reviewer helped improve the manuscript.

References

[1] Radulian M, Mândrescu N, Panza GF, Popescu E, Utale A. Characterization of seismogenic zones of romania. Pure and Applied Geophysics 2000;157:57–77.

[2] Oncescu M-C, Bonjer KP, Rizescu M. Weak and strong ground motion of intermediate depth earthquakes from the Vrancea region. In: Wenzel F, Lungu D, Novak O, editors. Vrancea Earthquakes: Tectonics, Hazard and Risk Mitigation. Kluwer Academic Publishers; 1999, p. 27–42.

[3] Wenzel F, Sperner B, Lorenz F, Mocanu V. Geodynamics, tomographic images and seismicity of the Vrancea region (SE-Carpatians, Romania). EGU Stephan Mueller Special Publication Series 2002;3:95–104.

[4] J. Miksat, Earthquake ground motion modelling from crustal and intermediate depth sources, Ph.D. Thesis, Karlsruhe University, 2006.

[5] Oth A, Bindi D, Parolai S, Wenzel F. S-Wave attenuation characteristics beneath the vrancea region in romania: new insights from the inversion of ground-motion spectra. Bulletin of the Seismological Society of America 2008;98:2482–97.

[6] Popa M, Radulian M, Grecu B, Popescu E, Placinta AO. Attenuation in Southeastern Carpathians area: result of upper mantle inhomogeneity. Tectonophysics 2005;410:235–49.

[7] Russo RM, Mocanu V, Radulian M, Popa M, Bonjer K-P. Seismic attenuation in the Carpathian bend zone and surroundings. Earth and Planetary Science Letters 2005;237:695–709.

[8] Enescu D, Marmureanu G, Enescu BD. A procedure for estimating the seismic hazard generated by Vrancea earthquakes and its application—II. Attenuation curves. Romanian Reports in Physics 2004;56:124–8.

[9] D. Jianu, Attenuation of intensity with distance for Vrancea intermediate earthquakes, in: Proceedings of ESC XXIII general assembly, Prague, Czechoslovakia, 1992, pp. 398–401.

[10] V.I. Marza and A.I. Pantea, Probabilistic estimation of seismic intensity attenuation for Vrancea (Romania) subcrustal sources, in: Proceedings of ESC XXIV General assembly, Athens, Greece, 1994, pp. 1752–1761.

[11] Sokolov V, Bonjer K-P, Wenzel F, Grecu B, Radulian M. Ground-motion prediction equations for the intermediate depth Vrancea (Romania) earthquakes. Bulletin of Earthquake Engineering 2008;6:367–88.

[12] Pantea AI. Macroseismic intensity attenuation for crustal sources on Romanian territory and adjacent areas. Natural Hazards 1994;10:65–72.

[13] Ardeleanu L, Leydecker G, Bonjer K-P, Busche H, Kaiser D, Schmitt T. Probabilistic seismic hazard map for Romania as a basis for a new building code. Natural Hazards and Earth System Sciences 2005;5:679–84.

[14] L. Ardeleanu, G. Leydecker, T. Schmitt, K.-P. Bonjer, H. Busche, D. Kaiser, et al., Probabilistic seismic hazard maps in terms of intensity for Romania and Bulgaria, in: Proceedings of International Symposium on Strong Vrancea Earthquakes and Risk Mitigation, Bucharest, Romania, October 2007.

[15] Zsíros T. Macroseismic focal depth and intensity attenuation in the Carpathian region. Acta Geodaetica et Geophysica Hungarica 1996;31:115–25.

[16] Sørensen MB, Stromeyer D, Grünthal G. Attenuation of macroseismic intensity - a new relation for the Marmara Sea region, NW Turkey. Bulletin of the Seismological Society of America 2009;99(2A):538–53.

[17] Stromeyer D, Grünthal G. Attenuation relationship of macroseismic intensities in Central Europe. Bulletin of the Seismological Society of America 2009;99(2A):554–65.

[18] Mândrescu N, Anghel M, Smalberger V. The Vrancea intermediate-depth earthquakes and the pecularities of the seismic intensity distribution over the Romanian territory. Studii si Cercetari de Geologie, Geofizica, Gergrafie, GEOFIZICA 1988;26:51–7.

[19] Oncescu M-C, Bonjer K-P. A note on the depth recurrence and strain release of large Vrancea earthquakes. Tectonophysics 1997;272:291–302.

[20] Räkers E, Müller G. The Romanian Earthquake of March 4, 1977—III. Improved focal model and moment determination. Journal of Geophysics 1982;50:143–50.

[21] Trifu C-I, Oncescu M-C. Fault geometry of August 30, 1986 Vrancea earthquake. Annales Geophysicae 1987;5B:727–30.

[22] Perrot J, Descamps A, Farra V, Virieux J. A 2-D velocity model of the Vrancea region in Romania: prediction of teleseismic waveforms. Geophysical Journal International 1996;125:537–44.

[23] J. Tavera, Études des mécanismes focaux de gros séismes et sismicité dans le région de Vrancea–Roumanie, Rap. Stage DEA Géophys Interne, Institut de Physique du Globe de Paris, France, 1991.

[24] G. Grünthal (Ed.). European Macroceismic Scale 1998 (EMS-98). Cahiers du Centre Europeén de Géodynamique et de Séismologie, vol. 15, 99 pp., Luxembourg, 1998.

[25] Sørensen MB, Stromeyer D, Grünthal G. Intensity attenuation in the Campania region, Southern Italy. Journal of Seismology 2010;14:209–23.